



Natural radioactivity due to uranium and radon in thermal groundwaters of Central Brazil

M. Lunardi¹ · D. M. Bonotto¹

Received: 16 September 2022 / Accepted: 11 January 2023 / Published online: 30 January 2023
© Akadémiai Kiadó, Budapest, Hungary 2023

Abstract

Hot springs from the Caldas Novas Thermal Complex have been used for balneological purposes since its discovery in the eighteenth century. A detailed analysis has been conducted to investigate the natural radioactivity of these waters due to dissolved ^{222}Rn , ^{238}U and ^{234}U . Sampling campaigns occurred during the dry and rainy seasons to observe how these radioelements are affected by seasonality. Measurements included analyses of alpha-emitting radionuclides, physicochemical parameters and major constituents. Aside from quantitative results, significant correlations were obtained between ^{222}Rn , dissolved oxygen, Eh and sodium, and between ^{238}U , dissolved oxygen, pH, electrical conductivity and calcium. The $^{234}\text{U}/^{238}\text{U}$ activity ratio was used as an indirect prospecting tool to indicate whether or not there are potential uranium ore bodies currently forming in this area, and also to demonstrate how mixing of different groundwater masses is occurring.

Keywords Natural radioactivity · Thermal groundwater · Uranium · Radon · Caldas Novas

Introduction

Naturally occurring radioelements can lead to serious health problems when present in high concentrations in drinking water. Radon in the air is the leading cause of lung cancer in nonsmokers and it somewhat increases the risk of stomach cancer when in the water [1], while health effects reported from uranium exposition include the impairment of organs such as kidneys and lungs [2]. Thus, it is essential to measure and report radioactive components in surface and groundwater at regular intervals of time.

Due to its high abundance among uranium isotopes (over 99%), ^{238}U is one of the most studied radioisotope in the water cycle, and its daughter product ^{222}Rn is the radon isotope of most interest. A regulatory limit of 30 $\mu\text{g}/\text{L}$ for ^{238}U is adopted in many countries [3–7], whereas for ^{222}Rn there is still a lack of standardization. Several countries, mostly located in Latin America and Asia, have no regulatory limit for the presence of radon in air or water [8]. Currently, there are no set standards or laws concerning radon in water in the United States also, but the Environmental Protection

Agency (EPA) recommends drinking water standards for radon in water ranging from 300 to 10,000 pCi/L (circa 11–370 Bq/L) [9, 10]. On the other hand, a more stringent control policy was adopted in Europe, lowering the reference level for radon in water to 100 Bq/L [11]. In Brazil, radioactivity in waters due to radon are given in Mache Unit, UM (1 UM = 13.45 Bq/L), an obsolete unit of volumetric radioactivity. The Brazilian Mineral Water Code establishes that: waters will be considered slightly radioactive if containing 5–10 UM, radioactive if containing 10–50 UM and strongly radioactive if containing over 50 UM [4].

Recently, researchers have identified specific workplaces where higher levels of radon are expected, such as mines, touristic caves, water treatment facilities and spas [12]. Godoy and Godoy [13] gathered natural radioactivity data from several water samples across the country, including hot springs samples from spas in Caldas Novas, and concluded that Central Brazil has the lowest values of uranium and radon. Nevertheless, radon measurements reported by Campos et al. [14] pointed out a value of 18.5 UM in one of the hot springs from the Caldas Novas Thermal Complex, classifying it as radioactive.

Some parameters can oscillate over time so that, within a region with fairly uniform rock types, some wells exhibit concentrations far above the average for that region, beyond that significant seasonal variations in concentrations can

✉ D. M. Bonotto
daniel.bonotto@unesp.br

¹ UNESP-São Paulo State University, Rio Claro 13506-900, Brazil

also be observed [11]. However, far too little attention has been paid to radioactivity in Caldas Novas' hot springs. That being the case, this study aimed provide an insight of uranium and radon in waters during two different seasons to comprehend how these radioelements are affected.

Radon in water

Surface waters are submitted to turbulence promoted by environmental factors, favoring for radon to easily escape into the environment. For this reason, rivers and streams tend to have low concentrations of this radioelement [15, 16], usually well below 1 Bq/L, while concentrations in groundwater vary from 1 to 50 Bq/L in sedimentary rocks, to 10–300 Bq/L for wells dug in soil, and to 100–50,000 Bq/L in crystalline rocks [11].

Because radon is an inert gas, it moves rather freely through porous media such as soil or fragmented rock. In pores saturated with water, as in soil and rock under the water table, radon is dissolved into the water and transported by it [11]. However, only a certain percentage of radon atoms emanated from rocks are released and mobilized because, during the decay process from ^{226}Ra , ^{222}Rn formed is propelled away from the site of decay and an alpha particle recoils in the opposite direction. Depending on its position and orientation in a mineral, ^{222}Rn may either end up in water-filled fractures or be buried deeper in the rock matrix [17, 18]. The recoil distance is dependent on the material's density and composition but the diffusion length of ^{222}Rn is generally short (0.02–0.07 mm) [19], so only a few millimeters of the rock layer near fractures can potentially contribute to an increase of radon concentration in water.

Uranium in water

In the hydrological environment, uranium is insoluble under reducing conditions and soluble mainly in the form of uranyl complexes (UO_2^{2+}) that pair with commonly dissolved anions in waters [20]. In natural waters, uranyl complexes bond with fluorine under acidic conditions (pHs between 2 and 4), phosphate in more neutral conditions (pHs between 4 and 7.5), and carbonate under alkaline conditions, with smaller contributions of sulfate and chlorine [21]. Bicarbonate is the dominant anion in most waters so, at typical groundwater CO_2 pressure (10^{-2} atm at 25 °C for $\text{pH} > 5$), uranyl carbonate complexes are found to be the main species in solution.

Isotopes ^{234}U and ^{238}U are generally found in radioactive disequilibrium in surface waters and groundwater. This disequilibrium results from water–rock interaction and the recoil process suffered by the ^{234}Th alpha emitting nucleus that displaces ^{234}U out of the mineral, resulting in activity ratios greater than unity. During the displacement, uranium oxidizes to the hexavalent form, favoring its leaching from

rock to water [22]. Therefore, the enhancement of ^{234}U in solution increases with the degree of weathering in the aquifers, because high AR values are directly related to higher values of dissolution rate [23].

Study area

The Caldas Novas Thermal Complex is situated at southeast of Goiás State in Brazil, distant about 170 km of its capital Goiânia and 350 km far from Brasília, the country capital. The thermal waters of this complex comprise a large area in which are located the cities of Caldas Novas and Rio Quente, 35 km away from each other (Fig. 1).

Brazil has significant uranium resources, leading the country to occupy a prominent position in the world rankings among the top ten countries with the highest potential for uranium, along with Australia, Kazakhstan, Canada, Russia, Namibia, South Africa, China, and Niger [24, 25]. The most notable Brazilian uranium deposits are hosted by metasomatites, consisting of unevenly disseminated uranium in structurally deformed rocks that were affected by sodium and/or potassium metasomatism, and by the metamorphites, occurring in metasediments and/or metavolcanics unrelated to granite (e.g. Itatiaia's marble-hosted phosphate deposit) [26, 27]. Although metamorphites are one of the main rocks in the Caldas Novas Thermal Complex, there is no evidence so far of ore deposits in this area. The high temperatures of those hot springs, once investigated for possible links to radioactivity [28], are in fact product of severely deformational dynamics during the *Brasiliano* Cycle.

The complex geology in the Caldas Novas Thermal Complex is due to its intricate structural evolution. According to Campos et al. [29], it is possible to divide rocks into three main groups, the metamorphites attributed to the Paranoá and Araxá groups, and subordinate occurrences of conglomerates attributed to the Areado Group. In the study area, the Paranoá Group (Meso/Neoproterozoic) is represented by the Caldas Novas Dome and is subdivided into four lithostratigraphic units, from base to top: Orthoquartzite, Clay Quartzite, Metarrhythmite and Pelito-Carbonated. The Araxá Group (Neoproterozoic) corresponds to the flat region surrounding the dome, and its rocks are monotonous platform sequences metamorphosed into greenschist facies, with muscovite-quartz-biotite schists, muscovite-biotite schists, muscovite-biotite-garnet schists. Conglomerates belonging to the Areado Group (Early Cretaceous) occur along the eastern and western edges on top of the dome.

Campos et al. [29] synthesized the geological evolution of this area with the following historical moments. Starting with the deposition of a thick sedimentary column in the Paranoá Basin (Meso/Neoproterozoic) followed by the deposition of the Araxá Group (Neoproterozoic) under continental shelf conditions. Both sediments were later

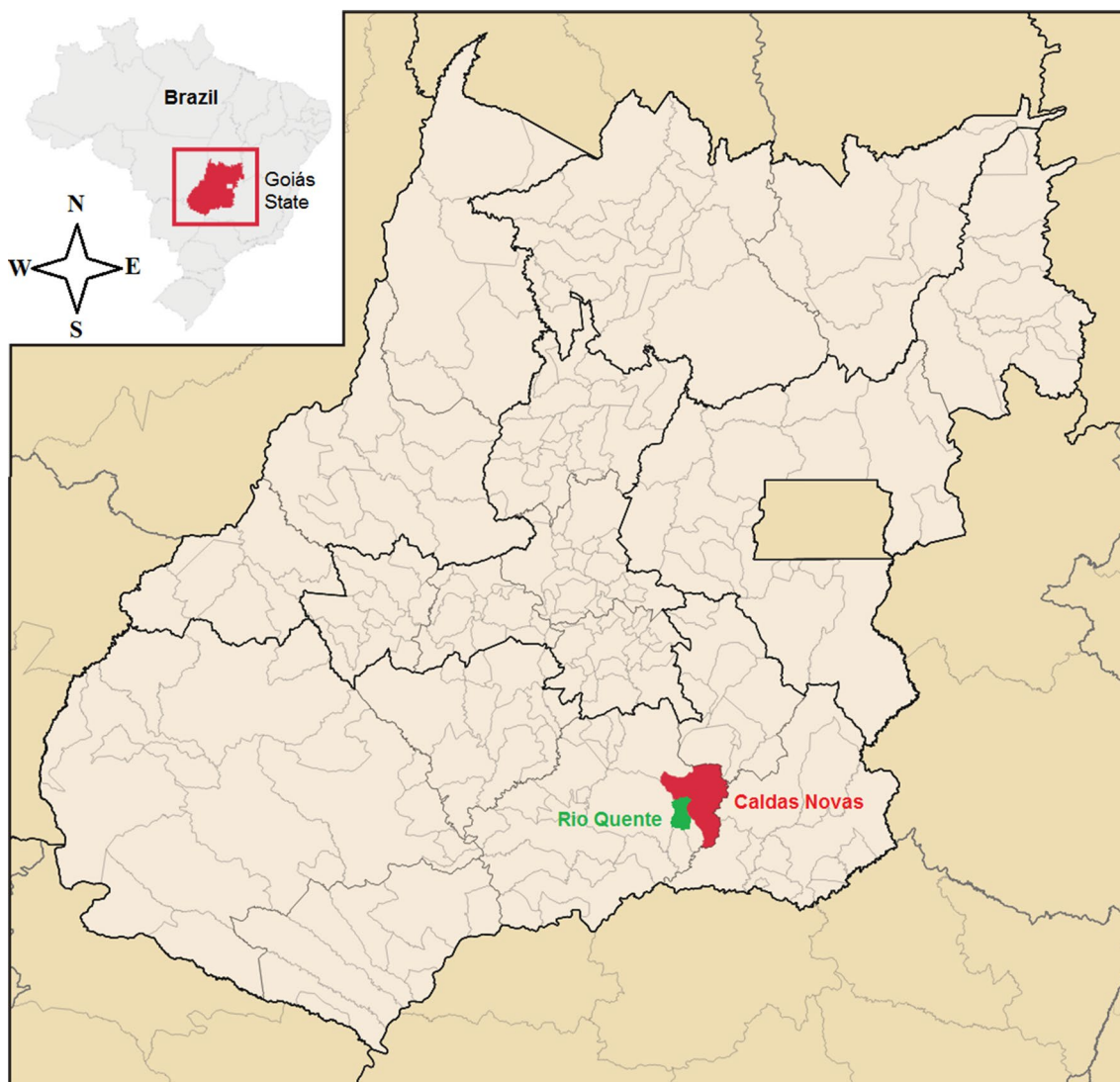


Fig. 1 Simplified map of location of Goiás State in Brazil, highlighting the municipalities of Caldas Novas (red) and Rio Verde (green). (Color figure online)

metamorphised, developing a nappe feature that puts the Araxá unit over the Paranoá Group and structuring the dome's NS axis during the *Brasiliano* Cycle. The dome was then uplifted with the structuring of the EW axis in the late stages of the Brazilian Cycle. Fracturing/folding events took place in the whole region (Araxá and Paranoá groups) in the *Brasiliano* Orogeny final stages. During the Cretaceous, there was normal reactivation of the planar structures by extensive tectonics, forming small rejects faults and enlarging the opening of existent fractures. In the Cenozoic, the schist's layers eroded while the most

resistant rocks (Paranoá Group) maintained their shape resulting in the relief observed nowadays.

Sampling and analysis

The sampling points of this study are shown in Fig. 2, while Figs. 3, 4 and 5 illustrate some pictures of the sampling sites. Most sampling locations are spas, and thus private property, requiring the owner's consent to proceed. The Hot Park sampling location was chosen for being a key spot in Rio Quente, known as one of the biggest resorts in Brazil where numerous springs naturally ascend directly from the ground.

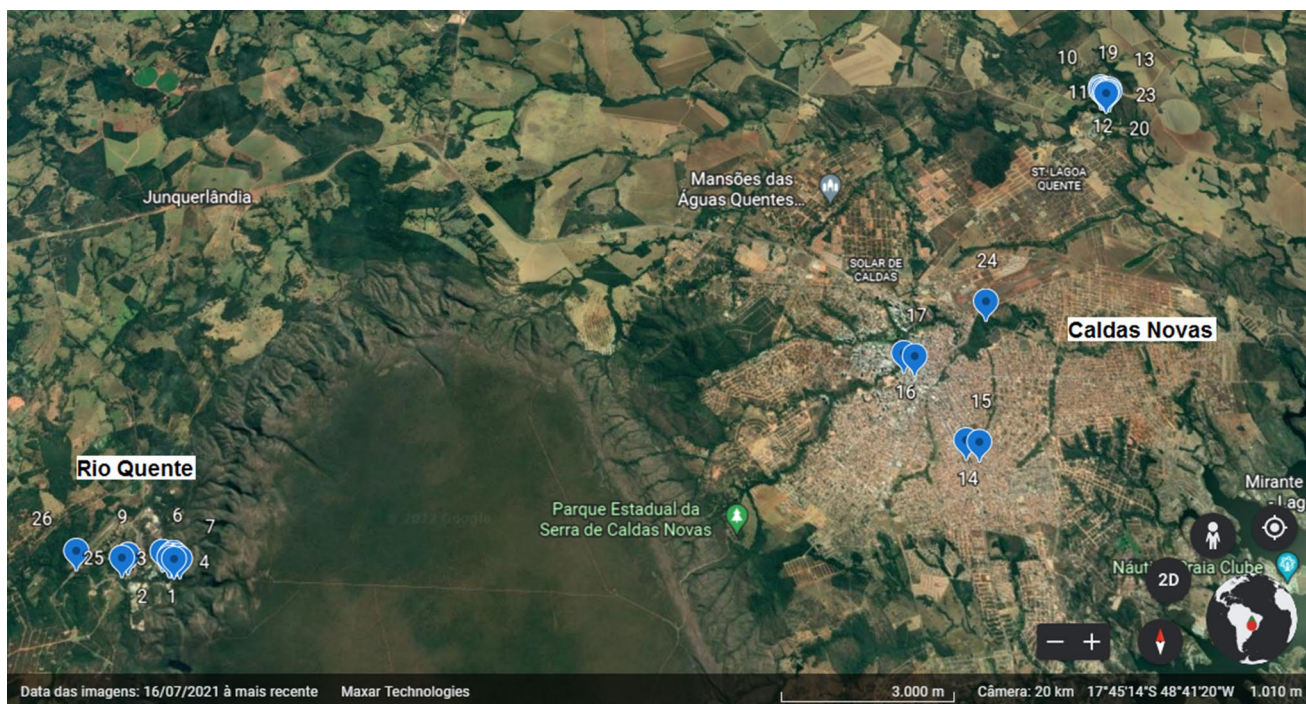


Fig. 2 Point map with the approximate location of sample collection places, taken from Google Earth (July/2021)



Fig. 3 (Left) Hatchway built to protect the spots where hot springs rise through fissures and cracks in the ground, inside the Rio Quente Resorts domains. (Right) The so-called “Spring’s Gutter” sampling

spot. It carries the waters from the whole park and forms a hot river that flows into the nature, after proper treatment, receiving the name of “Rio Quente”, portuguese for “Hot River”

Caldas Novas, on the other hand, has countless hotels and resorts, most of which dug wells to reach the thermal aquifers, so that the choice of the sampling spots was based solely on the owner’s authorization. Samples were collected directly from springs in two separate sampling campaigns to analyze how seasonality affects parameters. One campaign took place in November 2014 (rainy season), while the other occurred in May 2018 (dry season), altogether comprising

13 samples in each fieldwork, among which one rainwater and three surface water samples were also collected.

Generally, in waters, the highest concentrations of dissolved radionuclides are associated with groundwaters, especially those confined in deep aquifers as their contact with the radioactive elements occurring in the rocks is longer. This is because the dissolution of natural radionuclides occurs slowly, lasting hundreds to thousands of years [30].



Fig. 4 (Left) Sampling performed in a few hot springs with open access to the public. (Right) Sampling in one of the springs from the Hot Lagoon Park, in the outskirts of Caldas Novas city. These springs are locally known as “the egg-cooker wells”, due to their high temperatures

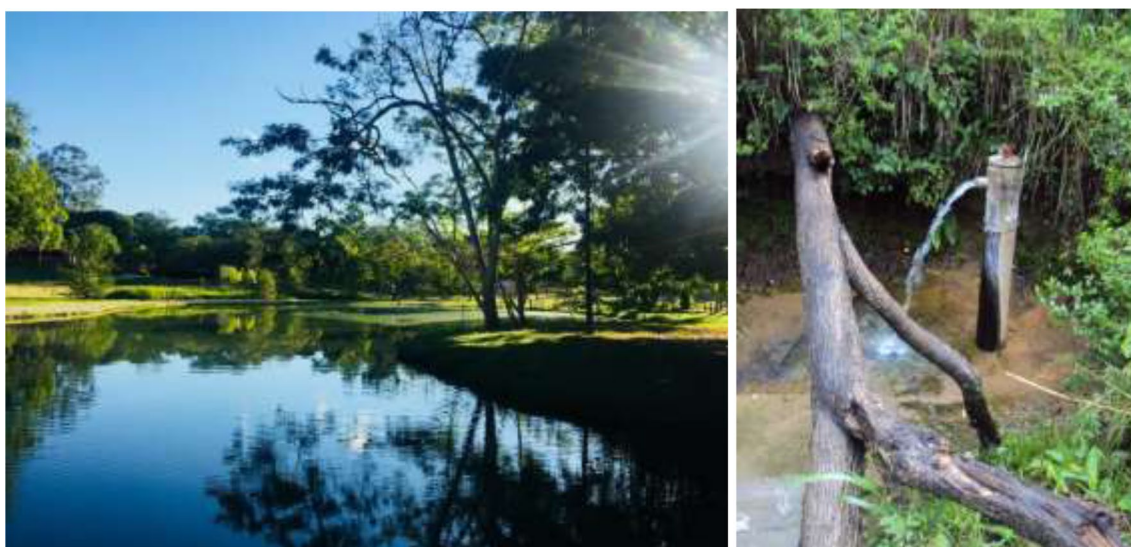


Fig. 5 (Left) The “Hot Lagoon” or “Pirapitinga Lagoon” sampling spot is one of the hottest springs from Caldas Novas, and lends its name to the park where is located. It is known to be the birth place of the thermal complex where pioneers first discovered the hot water

anomaly in the early eighteenth century. (Right) The so-called “Sulfur Spring” is located in central Caldas Novas city, in one of the banks of Caldas Stream, and has a characteristic rotten egg odor

Measurements of natural radioactivity of uranium and radon were also accompanied by readings of the physico-chemical parameters (temperature; pH; potential redox, Eh; electrical conductivity, EC; dissolved oxygen, DO) and other constituents (Na^+ , K^+ , Ca^{2+} , Mg^{2+} , total Fe, Cl^- , F^- , SO_4^{2-} , NO_3^- , PO_4^{3-} , CO_3^{2-} , HCO_3^- , SiO_2 and Tannin/Lignin). Water samples were stored in polyethylene bottles and the readings of temperature, pH, Eh, EC and DO were immediately performed, because its properties might change during transportation to the laboratory.

Temperature readings were done with a digital portable thermometer, while DO and EC data were obtained with the

handset Hanna (Model HI 9146) and Analion (Model C-702) meters, respectively. Protonic (pH) and electronic (Eh) activity determinations were made with a portable digital multi-parameter equipment from Digimed (Model DM-2P). The pH was measured coupling the meter to a glass electrode. The Eh measurement was realized with the same device after disconnecting the pH electrode, selecting the “mV” position, and connecting a combination Pt electrode–Ag/AgCl reference element. Such electrode was previously calibrated with a prepared Zobell I reference solution (Eh = 196 mV at 26.3 °C). This value, added to the half-cell potential (electromotive force = 230 mV), yielded 426 mV, which was very

close to the expected Eh value of 428 mV. Thus, there was no need to correct the Eh's field readings.

The chemical and radionuclides analysis of the water samples was carried out at LABIDRO-Isotopes and Hydrochemistry Laboratory in the Geology Department of the IGCE-Institute of Geosciences and Exact Sciences at UNESP-São Paulo State University in Rio Claro city. To analyze Na^+ and K^+ , a flame photometer from Benfer (Model BFC-300) was used by inserting the samples into a flame and analyzing the amount of radiation emitted by the excited ions according to characteristic wavelengths for each constituent. For the analysis of HCO_3^- and CO_3^{2-} , the acid titration method was adopted, allowing to determine the unknown amount of the ion by its reaction with a standard reagent: phenolphthalein in the case of CO_3^{2-} (at pHs < 8.3 the sample remains colorless, whereas at pHs above 8.3 the color shifts to pink) and, for HCO_3^- , a mixed indicator consisting of methyl red and bromocresol green, which changes from blue to salmon color.

Potentiometry was chosen to analyze F^- , using the selective fluoride electrode (Orion, Model No. 94-09) and a single junction reference electrode (Orion, Model No. 90-01) that were connected to the inputs of an ions analyzer for the potential readings. Standards containing variable concentrations of fluoride were utilized for preparing a calibration curve consisting on logarithmic straight lines involving the potential and concentration readings. The remaining chemical species were analyzed by the Hach spectrophotometer (Model DR/2000), a single-beam instrument, controlled by a microprocessor, used for colorimetric tests. The sample analysis started with the sample preparation, a simple procedure that consisted of adding the contents of sachets with pre-measured powder reagents, resting in 25 mL of the sample. After a certain resting time, another bottle containing 25 mL of the same water sample, called "blank", was placed in the reading compartment for the device to memorize a solution with value equivalent to 0.0 mg/L of the analyzed chemical species. After reading the blank, the solution containing the reagent was placed in the spectrophotometer reader so that the value of the chemical species present in the water sample could be determined.

Radon analyses were carried out on ^{222}Rn , the radon isotope with the longest half-life (3.82 days), which gives this radionuclide the ability to migrate greater distances from its origin [20]. Radon analyses of samples 1–13 (dry season) were first performed in the field, immediately after sampling, using the RAD7, a portable equipment that has a solid-state alpha particle detector that converts the alpha particle energy directly into an electrical signal [31]. Samples 14–26 (rainy season) were analyzed by the AlphaGuard equipment [32], a radon monitor that is a continuous active radon sampling sensor. It has an ionization chamber and also uses alpha spectroscopy to detect radon [33]. Both radon meters were

supplied calibrated by their respective manufacturers, while the performance was checked using the ^{226}Ra standard SRM No. 4969 (activity = 4 Bq/g) as provided by NIST-National Institute of Standards and Technology, Gaithersburg, Maryland, USA. Four ^{226}Ra solutions of activity corresponding to 17.5 ± 1 Bq were prepared from this standard in order to realize the ^{222}Rn analysis, which was done after about 25 days, i.e. the time required for ^{222}Rn to reach radioactive equilibrium with ^{226}Ra . The difference between the expected and measured results varied between 3 and 5%.

When radon decays inside the equipment's sampling cell, its nucleus turns into ^{218}Po remaining adhered to the detector surface. As the decay series continues, alpha radiation is released, producing electrical signals proportional to the energy. Different isotopes emit different alpha decay energies and consequently produce different electrical signals. The RAD7 spectrum is a scale of alpha particles energies from 6 to 9 MeV corresponding to the radon daughters deposited on the surface of the solid state detector, which produces an electrical signal that is converted to digital form. RAD7's microprocessor picks up the signal and stores it in its memory according to the energy of the alpha particle. Peaks in windows A and C come from new and old radon, respectively. Window A, for example, covers the energy range of 5.40–6.40 MeV, so it includes the 6.00 MeV alpha particle from ^{218}Po [31].

There are certain struggles in deriving activity concentrations of radon in drinking water because of the ease with which radon is released from water during handling [34]. To determine ^{222}Rn in water, the accessory RAD-H₂O was used, employing an aeration system in a closed circuit. RAD7's internal air pump circulates air at a 1 L/min rate, extracting ^{222}Rn until the radon-air-water equilibrium state develops. The system reaches equilibrium in about 5 min with an extraction efficiency of 94% for a 250 mL sample [35]. After 27 days, the second reading of radon was performed to determine the radium concentration in the samples, as within this time ^{222}Rn reaches radioactive equilibrium with its progenitor ^{226}Ra .

RAD7 makes readings either for real-time monitoring or sniffing. Sniffing means taking quick, spot readings, so one can get a rough idea of the radon level. This method is not affected by the exposure to high radon levels because it looks only at the ^{218}Po decays and ignores the ^{214}Po decays left over from previous sniffs. The ^{218}Po has a 3-min half-life, so the RAD7 sniffing for radon has a 15-min response time to both sudden increases and sudden decreases in level. Thus, the sniff mode shows that, for the present reading, only the ^{218}Po decays are being counted. Every five minutes, RAD7 prints out a paper report showing results of the measurement cycles along with a summary of the test. These paper reports display the measurement number, date and time, instrument serial number, number of cycles in the test, mean value,

standard deviation, the two-sigma statistical uncertainty, highest and lowest readings, a bar graph for the complete set of readings, a cumulative spectrum and also the temperature and humidity inside the measurement chamber. The bar graph shows the change in radon concentration in each measurement cycle while the cumulative spectrum shows the energy distribution of all alpha decays during the measurement. The radon content in the water at the time of analysis is the “Mean Value” shown on the paper report. This value is later adjusted because radon decay must be considered from the exact moment sampling occurred until analysis took place.

The AlphaGUARD device, employed for samples 14–26, has an extension that allows the reliable determination of radon in water, called AquaKIT. It is a series of accessories, mostly glassware, that directly measure radon in aqueous samples. The system also has a device called AlphaPUMP, comprising a pump responsible for pumping ^{222}Rn into the ionization chamber. Radon analysis in the water started by injecting 100 mL of sample into the emanation vessel. The device was then turned on at a flow rate of 0.03 L/min. For each sample, 30 min of measurement are required. In the first 10 min, suction is carried out through the pump and in the remaining 20 min the pump remains off to read the decay of radon activity [36]. Once the radon content is read, each water sample is taken and the device is cleaned with activated carbon. This process removes all radon from the AlphaGUARD system to avoid contamination of subsequent samples.

Isotopic analysis of uranium (^{238}U and ^{234}U) in the water samples followed the method described by Bonotto [20]. The alpha spectrometry technique was adopted for the isotopic analysis to characterize the uranium isotopes. This method uses stainless steel thin disks to avoid the absorption of alpha particles by the deposited layer. The samples were submitted to several steps, which involved [20, 37]: filtration of 20–25 L through 0.45 μm Millipore membranes; filtrate acidification until $\text{pH}=2$ with concentrated HCl (8 M); addition of ferric chloride (FeCl_3) and artificial radioactive tracer (^{232}U); pH raising to 7 or 8 with NH_4OH to precipitate ferric hydroxide [$\text{Fe}(\text{OH})_3$], which flocculates rapidly and “carries” the U-isotopes in its precipitation; precipitate recovery by centrifugation and dissolution in HCl (8 M) for generating uranyl chloride (UO_2Cl_2); Fe^{3+} separation from U-isotopes by extraction with isopropyl ether; evaporation of the acid layer containing uranium until dryness and dissolution into HCl (8 M) in order to form the complex ions (UO_2Cl_4) $^{2-}$ and (UO_2Cl_3) $^-$; separation of uranium from thorium and other elements in columns containing ion exchange resin; elution from the columns of uranyl chloride ions with 0.1 M HCl and evaporation to dryness; addition of H_2SO_4 (2 M) and $(\text{NH}_4)_2\text{SO}_4$ (2 M) electrolyte to the dry residue; transfer of the solution to an electrodeposition cell and adjust

of the pH to 2.4 using H_2SO_4 or NH_4OH ; carrying out the electrolysis under a constant current of 300 mA during 3 h and keeping a distance of 1 cm between the anode (Pt) and cathode (stainless steel disk); removal of the anode, disk washing with distilled water and disk drying under an infrared lamp; disk insertion in the vacuum chamber of the alpha spectrometer for reading with Si(Au) surface barrier detector. The detector was coupled to EG&G ORTEC multichannel buffer and the MAESTRO software allowed plotting the α -spectra containing the U-isotopes, according to the following sequence, based on the increase of the alpha particles energy, from left to right: peak 1 = ^{238}U (4.2 MeV), peak 2 (when present) = ^{235}U (4.4 MeV), peak 3 = ^{234}U (4.8 MeV), and peak 4 = ^{232}U (5.3 MeV). The analytical uncertainty was often between $\pm 10\%$ and $\pm 20\%$ at 1σ standard deviation, whereas the detection efficiency between 20 and 30%. The alpha spectrometric system was calibrated in energy using a radioactive source prepared at the *Centre de Faibles Radioactivités*, CNRS-CEA, Gif-sur-Yvette, France, and containing 0.91 Bq of ^{238}U . In addition, the same source included ^{234}U and 0.17 ± 0.1 Bq of ^{232}U . Occasional participation in Analytical Quality Control Services such as NUSIMEP provided by IRMM-Institute for Reference Materials and Measurements, European Commission, Joint Research Centre, Retieseweg, Geel, Belgium, has allowed to report reliable $^{234}\text{U}/^{238}\text{U}$ ratios in saline solutions.

Results and discussion

Results for physicochemical analysis and major constituents of the water samples are reported in Tables 1 and 2, respectively. Tables 3, 4 and 5 comprise the results of radon activity concentration while Table 6 gathers the results for dissolved uranium concentration and $^{234}\text{U}/^{238}\text{U}$ activity ratio (AR).

Dissolved radon relationships

Results for radon analysis in water during the dry season and obtained by the RAD7 equipment are reported in Tables 3 and 4. Table 3 shows the values of ^{222}Rn in Bq/L soon after sampling took place, while Table 4 shows the values of ^{226}Ra in Bq/L after radioactive equilibrium between ^{222}Rn and ^{226}Ra was reached 27 days later. The radon data for samples obtained during the rainy season and analyzed by the AlphaGUARD equipment are shown in Table 5.

In Brazil, there is no specific legislation for radon ingestion in drinking water, but the Brazilian Ministry of Health [3] recommends a limit for total alpha radiation of 0.5 Bq/L (including the isotope ^{226}Ra , the precursor of ^{222}Rn) and 1 Bq/L for total beta radiation. The Brazilian Code of Mineral Waters considers waters as weakly radioactive when

Table 1 Physicochemical parameters of the analyzed water samples

Sample	Campaign season	City	Sampling site	Water type	Temperature (°C)	Electrical conductivity ($\mu\text{S}/\text{cm}$)	Eh (mV)	pH	Dissolved oxygen (mg/L)	Total dissolved solids (mg/L)
1	Dry	Rio Quente	Hot Park—Spring 1	Groundwater	37.5	35	269	6.40	6.45	78.01
2	Dry	Rio Quente	Hot Park—Spring 2	Groundwater	37.5	36	270	6.22	6.20	49.11
3	Dry	Rio Quente	Hot Park—Spring 3	Groundwater	37.5	36	271	6.72	6.77	56.98
4	Dry	Rio Quente	Hot Park—Spring 4	Groundwater	37.5	35	273	6.36	6.66	55.28
5	Dry	Rio Quente	Hot Park—Spring 5	Groundwater	37.5	36	273	5.88	6.92	59.78
6	Dry	Rio Quente	Hot Park—Spring 6	Groundwater	37.5	38	273	6.45	6.81	58.45
7	Dry	Rio Quente	Fresh Fountainhead	Surface Water	29.0	25	244	6.70	6.95	45.80
8	Dry	Rio Quente	Spring's Gutter	Groundwater	37.0	36	253	6.50	6.98	58.51
9	Dry	Rio Quente	Esplanada Camping	Groundwater	26.5	38	238	7.00	6.92	54.19
10	Dry	Caldas Novas	Hot Lagoon Park	Groundwater	42.4	171	233	6.57	6.89	135.29
11	Dry	Caldas Novas	Hot Lagoon Park	Groundwater	41.3	169	228	6.38	6.97	139.59
12	Dry	Caldas Novas	Pirapitinga River	Surface Water	27.0	22	215	7.35	6.83	40.66
13	Dry	Caldas Novas	Hot Lagoon	Groundwater	26.5	148	240	6.87	6.84	153.03
14	Rainy	Caldas Novas	Costa Machado Inn	Groundwater	40.2	210	113	7.71	5.67	161.14
15	Rainy	Caldas Novas	Costa Machado Inn	Rainwater	22.9	58	181	6.42	nm	12.89
16	Rainy	Caldas Novas	CTC Hotel	Groundwater	40.4	110	133	7.11	5.17	159.44
17	Rainy	Caldas Novas	CTC Hotel	Groundwater	55.9	30	125	6.54	4.86	78.25
18	Rainy	Caldas Novas	Hot Lagoon Flat Hotel	Groundwater	43.3	220	105	7.73	5.13	163.67
19	Rainy	Caldas Novas	Hot Lagoon Park	Groundwater	46.9	210	158	7.83	5.61	163.40
20	Rainy	Caldas Novas	Hot Lagoon Park	Groundwater	48.0	220	179	7.89	4.99	158.32
21	Rainy	Caldas Novas	Hot Lagoon Park	Groundwater	40.8	200	190	8.02	5.76	175.65
22	Rainy	Caldas Novas	Hot Lagoon Park	Groundwater	48.1	210	196	7.66	5.30	170.76
23	Rainy	Caldas Novas	Pirapitinga River	Surface Water	24.8	41	203	7.51	6.57	33.48
24	Rainy	Caldas Novas	Sulphur Spring	Groundwater	28.6	190	0	7.82	4.23	106.41
25	Rainy	Rio Quente	Esplanada Camping	Groundwater	33.6	44	150	7.36	5.83	45.82
26	Rainy	Rio Quente	Hot River	Groundwater	32.7	48	114	7.65	5.90	43.27

nm not measured

Table 2 Chemical analysis (in mg/L) of the analyzed water samples

Sample	Na ⁺	K ⁺	Ca ²⁺	Mg ²⁺	Total Fe	Cl ⁻	SO ₄ ²⁻	NO ₃ ⁻	PO ₄ ³⁻	CO ₃ ²⁻	HCO ₃ ⁻	SiO ₂	Tan/Lig	F ⁻
1	8.37	14.93	2.5	0.2	0.040	10.7	<1	0.3	0.58	<0.1	18	18.8	<0.1	0.79
2	0.23	1.29	1.3	1.4	0.037	1.1	1	0.3	0.65	<0.1	22	14.8	<0.1	0.36
3	0.46	1.06	7.3	3.4	0.050	0.2	1	1.2	0.58	<0.1	22	15.8	0.1	0.89
4	1.15	1.17	7.6	2.7	0.190	0.3	<1	1.0	0.66	<0.1	18	16.2	0.2	0.02
5	1.84	1.41	6.8	2.7	0.221	0.2	<1	1.1	0.63	<0.1	22	16.3	0.2	0.10
6	1.61	1.25	8.9	1.9	0.174	0.1	1	0.4	0.64	<0.1	18	15.5	0.4	0.05
7	1.61	0.82	5.8	2.3	0.940	0.3	1	0.4	0.30	<0.1	14	11.2	0.1	0.52
8	1.61	1.13	9.0	3.2	0.038	0.3	<1	0.8	0.63	<0.1	20	15.1	<0.1	0.11
9	0.69	0.86	4.6	2.4	0.049	0.6	1	1.0	0.65	<0.1	26	15.2	<0.1	0.09
10	1.84	3.01	2.1	7.4	0.187	0.2	1	0.2	0.01	<0.1	94	21.6	<0.1	0.49
11	1.84	2.89	1.9	8.0	0.209	0.5	1	0.7	0.04	<0.1	98	20.8	<0.1	0.29
12	1.15	0.55	2.7	1.3	0.976	0.4	<1	0.4	<0.01	<0.1	18	5.7	<0.1	0.17
13	2.30	2.58	26.0	10.0	0.077	1.2	1	0.4	0.01	<0.1	86	21.6	<0.1	0.24
14	1.50	2.00	18.5	10.2	0.007	<0.1	1	0.3	0.01	<0.1	116	6.0	<0.1	0.04
15	0.10	1.30	0.4	0.1	0.001	<0.1	<1	1.4	0.01	<0.1	5	1.7	<0.1	0.02
16	2.00	2.20	20.2	10.4	0.001	2.1	1	1.7	0.08	<0.1	112	6.7	<0.1	0.05
17	0.70	1.60	7.3	4.2	0.004	<0.1	1	1.2	0.52	<0.1	50	8.6	<0.1	0.04
18	2.00	2.40	21.8	7.5	0.006	<0.1	1	1.1	0.01	<0.1	117	9.9	<0.1	0.04
19	1.30	2.30	21.6	7.5	0.004	<0.1	1	1.1	0.02	<0.1	113	13.9	<0.1	0.04
20	1.30	2.30	21.8	7.6	0.010	0.3	1	1.1	0.05	<0.1	113	8.4	<0.1	0.04
21	1.60	2.00	22.0	7.5	0.005	0.2	1	1.1	<0.01	<0.1	119	19.0	<0.1	0.04
22	1.50	1.90	21.9	7.7	0.001	0.3	1	1.1	0.02	<0.1	119	16.2	<0.1	0.04
23	1.70	1.10	1.7	0.7	0.008	0.3	1	1.4	0.01	<0.1	17	5.5	0.1	0.03
24	8.50	1.70	11.2	0.9	0.001	1.0	8	1.1	0.02	<0.1	60	10.6	<0.1	0.05
25	0.30	0.70	3.1	1.8	0.001	<0.1	1	1.1	0.59	<0.1	25	7.5	<0.1	0.04
26	0.70	0.70	3.6	1.9	0.019	<0.1	1	1.3	0.60	<0.1	26	6.0	<0.1	0.05

Table 3 Activity concentration of ²²²Rn in the analyzed water samples

Sample	First reading	Hour	Maximum (Bq/m ³)	Mean (Bq/m ³)	Minimum (Bq/m ³)	Activity concentration (Bq/L)
1	10/05/2018	15 h 09	4110 ± 834	3100 ± 673	1380 ± 512	3.10 ± 0.67
2	10/05/2018	15 h 28	7550 ± 1110	6570 ± 996	4630 ± 883	6.57 ± 1.00
3	10/05/2018	15 h 45	9760 ± 1270	8770 ± 1185	7290 ± 1100	8.77 ± 1.18
4	10/05/2018	16 h 03	11,600 ± 1390	10,300 ± 1305	8960 ± 1220	10.30 ± 1.30
5	10/05/2018	16 h 23	12,100 ± 1420	11,900 ± 1410	11,700 ± 1400	11.90 ± 1.41
6	10/05/2018	16 h 40	9390 ± 1260	9040 ± 1230	8440 ± 1200	9.04 ± 1.23
7	10/05/2018	nm	nm	nm	nm	nm
8	10/05/2018	14 h 55	761 ± 401	507 ± 304	103 ± 207	0.51 ± 0.30
9	10/05/2018	16 h 55	6060 ± 1030	5520 ± 987	5110 ± 944	5.52 ± 0.99
10	10/05/2018	17 h 47	2050 ± 620	1890 ± 591	1610 ± 562	1.89 ± 0.59
11	10/05/2018	18 h 09	2360 ± 661	2090 ± 617	1710 ± 574	2.09 ± 0.62
12	10/05/2018	18 h 28	2200 ± 636	1860 ± 600	1640 ± 564	1.86 ± 0.60
13	10/05/2018	17 h 26	2710 ± 711	2290 ± 638	1620 ± 565	2.29 ± 0.64

nm not measured

Table 4 ^{226}Ra activity concentration obtained from ^{222}Rn measured in waters 27 days after sampling, when equilibrium between radon and its progenitor ^{226}Ra was reached

Sample	Second reading	Hour	Maximum (Bq/m^3)	Mean (Bq/m^3)	Minimum (Bq/m^3)	Activity concentration (Bq/L)
1	06/06/2018	11 h 06	138 ± 223	80.3 ± 194	34.4 ± 166	0.0803 ± 0.19
2	06/06/2018	11 h 25	138 ± 223	91.8 ± 205	68.8 ± 188	0.0918 ± 0.20
3	06/06/2018	15 h 09	68.8 ± 188	45.9 ± 163	$<0.1 \pm 138$	0.0459 ± 0.16
4	06/06/2018	15 h 28	138 ± 223	68.8 ± 194	34.4 ± 166	0.0688 ± 0.19
5	06/06/2018	15 h 46	34.4 ± 166	22.9 ± 152	$<0.1 \pm 138$	0.0229 ± 0.15
6	06/06/2018	16 h 05	68.8 ± 188	34.4 ± 163	$<0.1 \pm 138$	0.0344 ± 0.16
7	06/06/2018	16 h 25	34.4 ± 166	34.4 ± 166	34.4 ± 166	0.0344 ± 0.17
8	06/06/2018	16 h 43	68.8 ± 188	34.4 ± 163	$<0.1 \pm 138$	0.0344 ± 0.16
9	06/06/2018	17 h 01	68.8 ± 188	45.9 ± 163	$<0.1 \pm 138$	0.0459 ± 0.16
10	06/06/2018	17 h 19	34.4 ± 166	11.5 ± 152	$<0.1 \pm 138$	0.0115 ± 0.15
11	06/06/2018	17 h 38	34.4 ± 166	11.5 ± 152	$<0.1 \pm 138$	0.0115 ± 0.15
12	06/06/2018	17 h 56	34.4 ± 166	22.9 ± 152	$<0.1 \pm 138$	0.0229 ± 0.15
13	06/06/2018	18 h 14	$<0.1 \pm 138$	$<0.1 \pm 138$	$<0.1 \pm 138$	$<0.0001 \pm 0.14$

Table 5 Data for radon parameters in groundwater performed by the AlphaGuard equipment. Data modified from Lunardi [32]

Sample	Water temperature ($^{\circ}\text{C}$)	Radon value (Bq/L) ¹	Radon value (Mache Unit) ²
14	40.2	21.98 ± 2.89	1.717
15	nm	nm	nm
16	40.4	25.58 ± 3.03	1.998
17	55.9	8.79 ± 1.76	0.687
18	43.3	17.53 ± 2.40	1.369
19	46.9	9.30 ± 1.71	0.726
20	48.0	7.39 ± 1.55	0.577
21	40.8	3.04 ± 0.85	0.237
22	48.1	12.40 ± 1.92	0.968
23	nm	nm	nm
24	28.6	60.78 ± 5.54	4.747
25	33.6	1.10 ± 0.86	0.085
26	32.7	0.36 ± 0.16	0.028

¹Radon analysis results initially reported in Bq/m^3 by the AlphaGuard were converted to Bq/L

²Radon results in Mache Unit, the standard unit adopted by Brazilian Code of Mineral Waters that refers to radon radioactivity contained in a liter of water, without taking into account its decay products and assuming that all the alpha particles emitted were used, producing an ionization current equal to one thousandth of an electrostatic unit

nm not measured

containing radon activity concentration between 5 and 10 UM (~ 67.5 – $135 \text{ Bq}/\text{L}$) [4].

Radon activity concentrations from the dry season ranged from 0.51 to 11.90 Bq/L , which does not classify them as radioactive according to the Brazilian Code of

Table 6 Concentration of dissolved uranium and $^{234}\text{U}/^{238}\text{U}$ activity ratio in the water samples

Sample	Volume (L)	Counting time (s)	$^{234}\text{U}/^{238}\text{U}$ activity ratio (AR)	U ($\mu\text{g}/\text{L}$)
1	18.43	230,335.2	1.07	0.060
2	19.38	252,557.5	1.25	0.044
3	20.05	183,920.0	1.16	0.039
4	20.71	165,954.2	1.01	0.046
5	19.83	417,768.6	5.50	0.008
6	20.55	230,320.5	4.00	0.021
7	20.04	204,155.9	4.17	0.084
8	19.27	505,411.6	1.18	0.008
9	20.37	165,999.3	1.95	0.001
10	19.64	166,027.1	4.08	0.001
11	18.34	230,310.9	1.56	0.002
12	18.67	183,918.5	1.06	0.002
13	8.97	183,917.2	2.37	0.060
14	15.0	30,883.5	5.00	0.073
16	15.0	86,133.5	6.67	0.011
17	15.0	107,652.4	1.64	0.021
18	15.0	107,612.2	1.95	0.117
19	15.0	196,149.7	1.92	0.081
20	15.0	86,105.5	0.67	0.308
21	15.0	333,435.0	2.59	0.053
22	15.0	77,632.6	1.11	0.208
24	15.0	108,695.0	1.33	0.143
25	15.0	658,815.4	1.67	0.126
26	15.0	64,115.9	0.87	0.072

Analytical uncertainty ± 10 – 15% at 1σ standard deviation

Mineral Waters [4]. The highest values belong to samples collected at the Hot Park Resorts in Rio Quente, with activity concentrations ranging between 8.77 and 11.90 Bq/L. The radon data obtained in the rainy season ranged from 0.365 to 60.779 Bq/L. The highest value belongs to the so-called Sulphur Spring, indicating that these waters are almost in the weakly radioactive class [4].

Statistical tests involving the Pearson correlation coefficient and P -value have been applied to the acquired dataset. The Pearson correlation coefficient (denoted by r) is a measure of the strength of a linear association between two variables. Such coefficient expresses how far away the obtained dataset is from the adjusted best fit line. The Pearson values range from +1 to -1 , and its strength of association is considered weak between 0.1 and 0.3, moderate between 0.3 and 0.5 and strong between 0.5 and 1.0 [38]. The P -value is a hypothesis testing that expresses the level of statistical significance [39]. A P -value, or probability value, is a number describing how likely the data would have occurred by random chance (i.e. that the null hypothesis is true). The level of statistical significance is often expressed as a P -value between 0 and 1. The smaller the P -value, the stronger is the evidence that the null hypothesis should be rejected [40].

Figure 6a displays a negative correlation obtained between DO and radon activity concentration ($r = -0.64$; P -value = 0.0010). This result reveals a tendency of radon activity concentration to increase in progressively anoxic environments. It possibly relates to the fact that deeper confined aquifers have limited or no contact with the atmosphere, decreasing oxygen availability. Radon levels usually are higher in such environments because the escape of this highly volatile gas to the atmosphere is also limited.

Groundwater samples confined in oxygen-deficient regions will exhibit more negative Eh values than those in shallower groundwater that is closer to the contact with the oxidizing atmosphere. In aquifer systems, there is a trend that low Eh values are most common at high pH values, to the point that high Eh values are obtained mainly at low pH values. Therefore, the most commonly found characteristics are acidic oxidizing and basic reducing systems [20]. This was confirmed by the significant negative correlation between Eh and pH from data reported in Table 1 ($r = -0.68$ and P -value = 0.00001). As pH values increase by 1–2 units and the aqueous environment becomes progressively more alkaline, Eh values drop to up to one-third of the initial value.

Figure 6b shows a negative correlation obtained between Eh and radon activity concentration ($r = -0.66$; P -value = 0.0006). Waters from reducing environments (lower Eh), mostly collected in Caldas Novas city, tend to have higher concentrations of radon than oxidizing environments (higher Eh), a condition that prevailed in Rio Quente city samples. This aligns with results from Fig. 6a

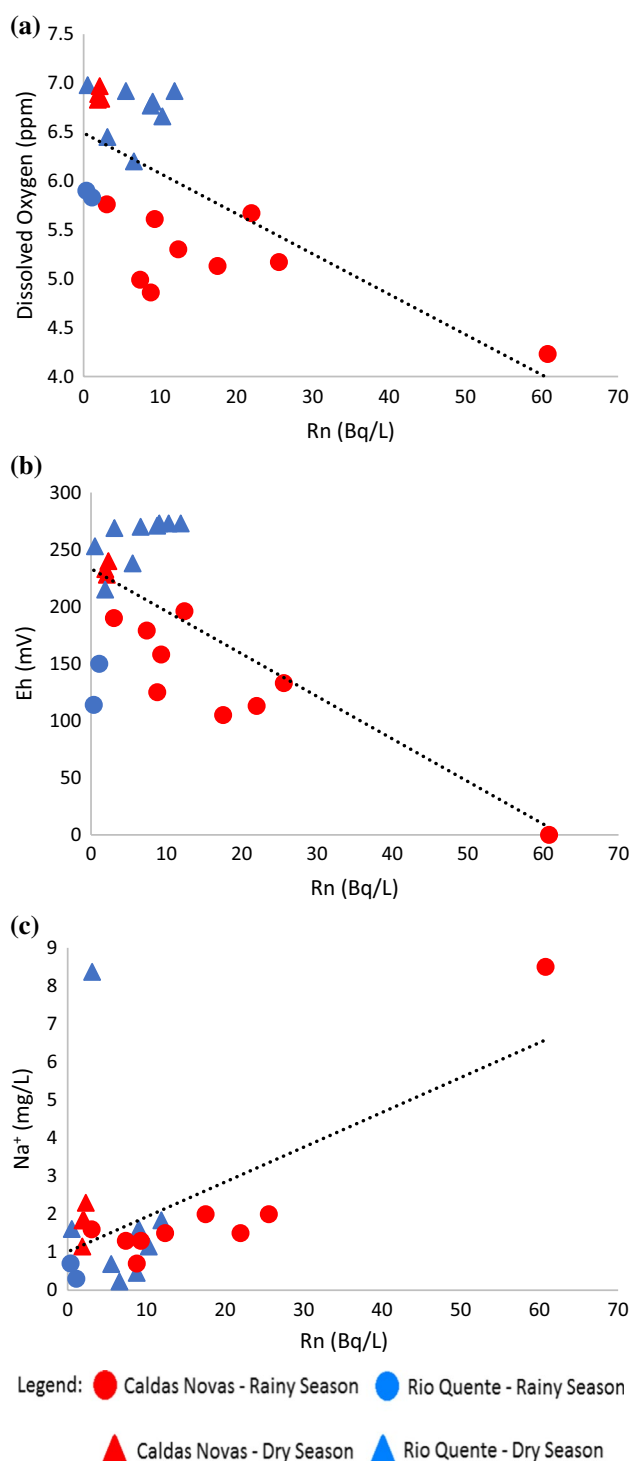


Fig. 6 Diagrams of radon relationships, showing negative correlations with **a** dissolved oxygen and **b** Eh, and **c** a positive correlation with Na⁺. These trends indicate that radon is directly influenced by anoxic and reducing environments, especially if in presence of sodium. (Color figure online)

since reducing environments are commonly associated with anoxic conditions, both found in deep confined aquifers regions. On the other hand, oxidizing groundwater refers to the water where DO is present. Since the atmosphere is the source of DO in water, these conditions relate to shallow aquifers near where recharge occurs, as observed for the Hot Park samples occurring alongside the main recharge area, the Caldas Novas dome.

Figure 6c exhibits a positive correlation obtained between sodium concentration and radon activity concentration ($r=0.56$; P -value=0.0057). Uranium is a lithophile element and concentrates preferentially in acid igneous rocks compared to intermediate, basic and ultrabasic varieties [41]. These rocks usually have higher sodium content and are characterized by also having a relatively high amount of rare elements. The richer a rock is in uranium the more radon it emits through decay processes. Although there are no strongly alkaline rocks such as syenites or phonolites in the Caldas Novas region, alkali-feldspars, plagioclases and tourmalines compose most of the metamorphic material and

are probably responsible for yielding a higher sodium content in a few samples. Most likely, such samples are originating from deeper confined regions of the aquifer where radon content is commonly higher. Another possibility relates to the geochemical evolution of groundwater, which suggests that ion exchange reactions might be occurring between sodium and calcium in clay minerals in deep waters in some regions of the aquifer system.

Dissolved uranium relationships

Results for uranium analysis were obtained through the alpha spectra that allowed to determine values ranging from 0.001 to 0.308 $\mu\text{g/L}$ as presented in Table 6, all far below the maximum allowed for U ingested in drinking water. The highest dissolved uranium concentrations are associated with groundwater samples that naturally have higher concentrations of this radioelement because the water–rock interaction in confined aquifer environments lasts longer, whereas in

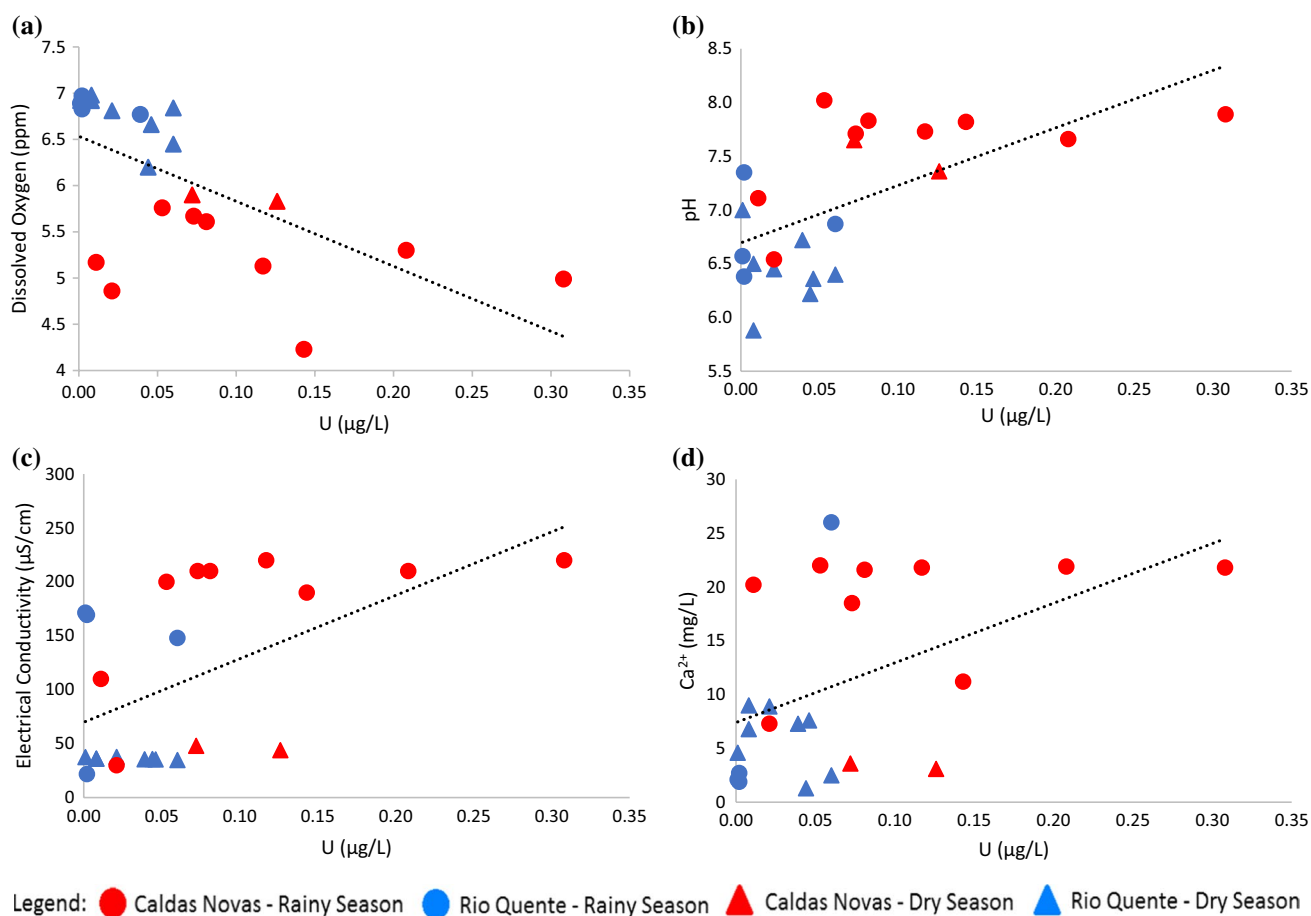


Fig. 7 Diagrams of uranium relationships, showing **a** a negative correlation obtained with dissolved oxygen, and positive correlations with **b** pH, **c** electrical conductivity and **d** calcium content, indicating that

anoxic environments favor uranium concentration, especially when pH ranges from neutral to slightly alkaline, and increasing EC and Ca^{2+} also contribute to increasing uranium levels. (Color figure online)

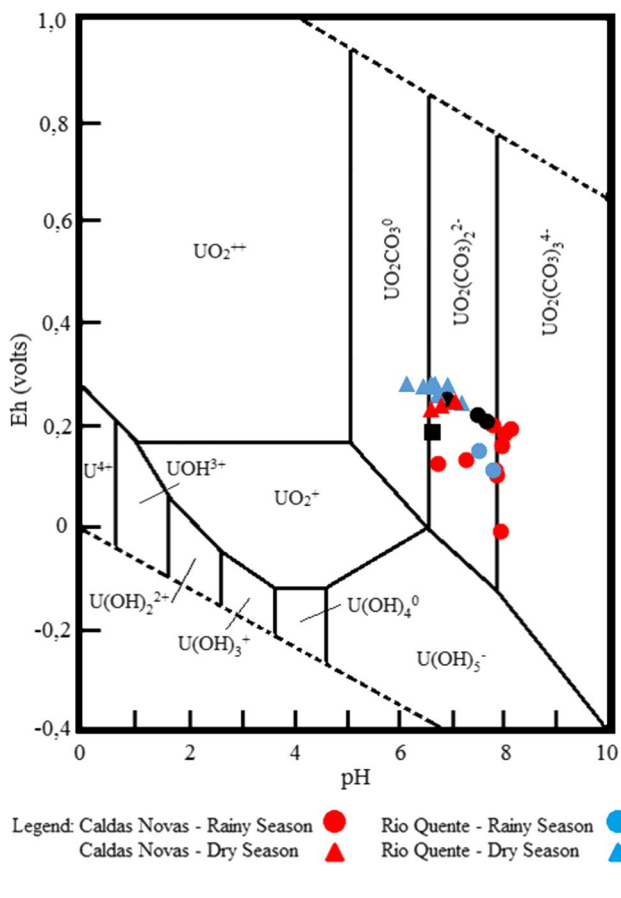


Fig. 8 Eh–pH diagram by Langmuir [42] showing that uranium species in waters from the Caldas Novas Thermal Complex are under the form of uranyl carbonate complexes. Red icons represent groundwater samples from Caldas Novas city while blue icons represent groundwater samples from Rio Quente city. The rainwater sample is marked by a black square and the black circles stand for the surface waters samples. (Color figure online)

surface water uranium is easily loaded from the rocks along with other weathering products.

Uranium exhibited significant correlations with physicochemical and chemical parameters (pH, DO, EC, Ca^{2+}) as displayed in scatter plots of Fig. 7. Data from uranium concentration (U) was plotted over an Eh vs. pH diagram as proposed by Langmuir [42] to show which uranium complexes are stable under the aquifer’s environment circumstances (Fig. 8). Data from U-isotopes was also used as a guide to prospecting, aiming to determine any possible accumulation of uranium in the aquifer’s vicinity. To do so, a plot of AR vs. uranium concentration (U) as proposed by Cowart and Osmond [43] was created (Fig. 9) to help identify redox fronts, locate uranium accumulations, and determine whether such accumulations are being augmented or depleted by contemporary aquifer/groundwater conditions. Figure 10 shows scatter plots correlating the inverse of uranium concentration ($1/U$) and AR to propose

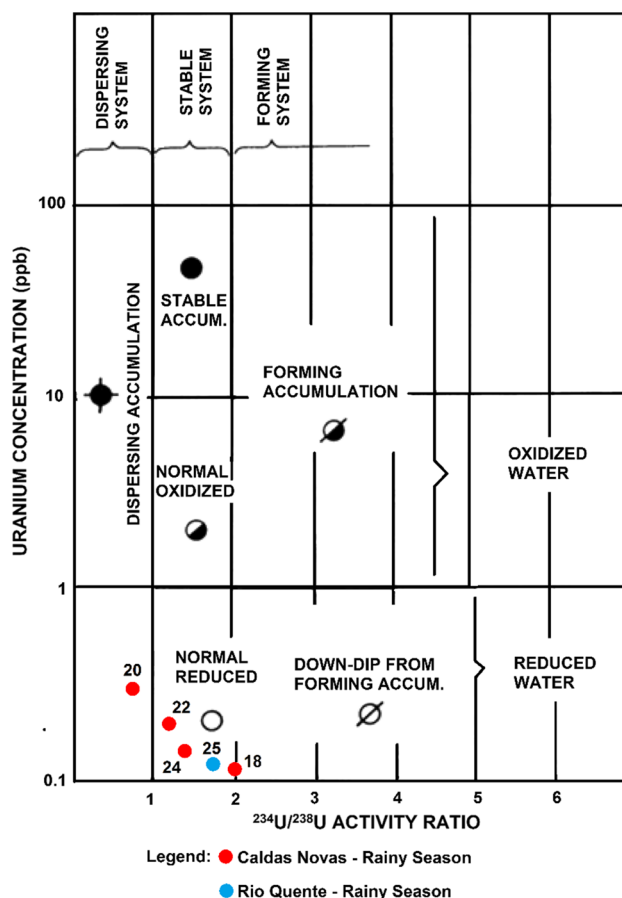


Fig. 9 Diagram of uranium concentration (ppb) vs. $^{234}U/^{238}U$ activity ratio (AR) as proposed by Cowart and Osmond [43], indicating that there are no potential uranium ore bodies currently forming by accumulation process from groundwater in the areas where samples were collected. (Color figure online)

how groundwater mixtures might be occurring in both cities in different seasons.

Figure 7a shows a negative correlation between uranium concentration and DO content in water ($r = -0.63$ and $P\text{-value} = 0.0012$). Several underground water reservoirs, such as the Caldas Novas Thermal Complex, have their origin in meteoric waters. These waters originate in the atmosphere, an environment endowed with unlimited oxygen. The partial pressure of oxygen exerted between the liquid and gas phases, according to Henry’s Law, allows water to contain a few ppm of DO. If some of this DO is consumed in reactions with the soil, rocks or vegetation, it will be constantly replenished. However, as meteoric water penetrates in progressively deeper layers of rocks and isolates itself from the atmosphere, there will be no more oxygen available in the underground environment after it has been consumed by reactions with adjacent rocks. Thus, more confined regions of the aquifers, where the waters are naturally richer in

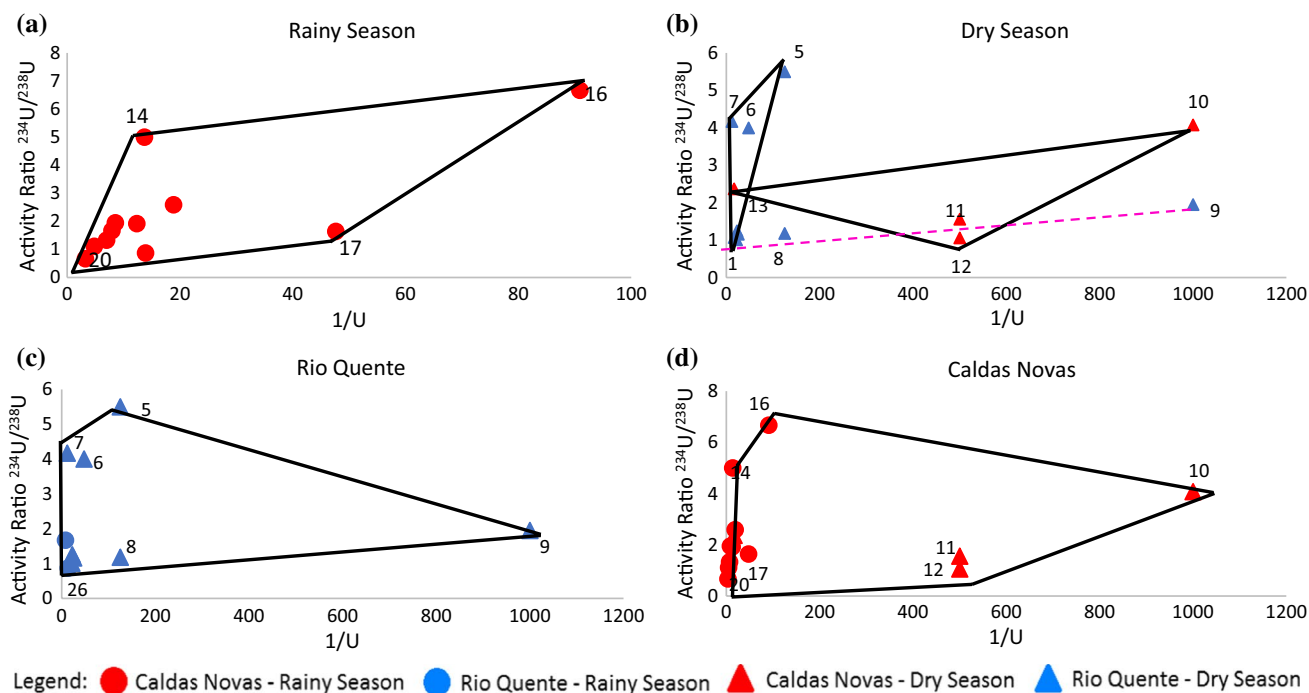


Fig. 10 Graphics of the $^{234}\text{U}/^{238}\text{U}$ activity ratio vs. inverse of uranium concentration ($1/U$) as proposed by Osmond et al. [48], showing the mixing volumes of different groundwater masses in the following scenarios: **a** during the rainy season, **b** during the dry season, **c** in Rio

Quente city and **d** in Caldas Novas city. Red icons stand for Caldas Novas's samples, while blue icons represent Rio Quente's samples. (Color figure online)

uranium, are also more anoxic environments. This explains the inverse correlation obtained in Fig. 7a, revealing that samples collected in Caldas Novas, where the waters reach greater depths, had the lowest levels of DO, while samples collected in Rio Quente, at depths relatively closer to the surface, obtained higher DO levels.

Figure 7b shows a positive correlation between uranium content and pH ($r=0.61$; $P\text{-value}=0.0018$), meaning that samples transitioning from neutral to alkaline pH, collected mostly in Caldas Novas city, had higher uranium contents than waters with more acidic tendencies, collected mostly in Rio Quente city. This might relate to the aquifer's confinement since groundwater in relatively deep and confined regions tend to be more alkaline and have higher concentrations of uranium due to residence time.

Figure 7c shows a positive correlation between the uranium concentration and EC ($r=0.55$; $P\text{-value}=0.0071$). Uranium content was higher in samples loaded with ionic species, most of them collected in Caldas Novas city, while samples collected in Rio Quente exhibit low values for both uranium and EC. This also correlates to the aquifer's depth and residence time, because deeper groundwater is exposed to rocks for a longer period. The more water–rock interactions happen, the more ionic species are carried into the solution, including uranium complexes, which increases EC values.

Figure 7d shows a positive correlation between calcium and uranium ($r=0.49$; $P\text{-value}=0.0173$). Waters from Caldas Novas city are also richer in both calcium and uranium due to a prolonged residence time, a hypothesis also sustained by pH and EC correlations. Although in most deep groundwater systems calcium tends to precipitate due to CaCO_3 saturation index or suffer exchange processes with sodium, in the Caldas Novas Thermal Complex these changes are not observed. Calcium is the dominant cation in most samples and its levels maintain a steady rise from shallower samples of Rio Quente city to deeper samples of Caldas Novas city. The highest calcium contents are linked to the highest uranium contents through a prolonged time of water–rock interaction.

The diagram of Fig. 8 shows stability fields for dissolved uranium species under different Eh and pH conditions. According to the diagram proposed by Langmuir [42], dissolved uranium in samples from the Caldas Novas Thermal Complex might occur as carbonate complexes [UO_2CO_3^0 , $\text{UO}_2(\text{CO}_3)_2^{2-}$ and $\text{UO}_2(\text{CO}_3)_3^{4-}$]. In most oxygen-rich environments absent of organic matter, carbonate complexes are likely to dominate uranium speciation. This happens because carbonates (CO_3^{2-}) have the ability to solubilize UO_2^{2+} , as carbonate complexes, thus, increasing the likelihood of uranium mobility in alkaline conditions [43]. This means in groundwater, under alkaline conditions, the dominant uranyl

complexes are formed with carbonates. The most likely uranyl-carbonate species to form is $\text{UO}_2(\text{CO}_3)_3^{4-}$, whilst $\text{CaUO}_2(\text{CO}_3)_3^{2-}$ and $\text{Ca}_2\text{UO}_2(\text{CO}_3)_3^0$ will form given that the solution has enough Ca^{2+} cations [44], which is the case. According to Baik et al. [45], Ca– UO_2 – CO_3 ternary complexes, $\text{CaUO}_2(\text{CO}_3)_3^{2-}$ and $\text{Ca}_2\text{UO}_2(\text{CO}_3)_3^0$ are expected to be significantly mobile in the geological media because they are thermodynamically stable in most of groundwater conditions and do not easily adsorb onto geological media [45]. Therefore, the results obtained are quite adequate and indicative of the greater influence that dissolved CO_2 has on the solubility of uranyl ions than (higher) pH alone [46].

U-isotopes relationships

The results of the $^{234}\text{U}/^{238}\text{U}$ activity ratio in this work ranged from 0.67 to 6.67, while the uranium concentration ranged from 0.001 to 0.308 $\mu\text{g}/\text{L}$ (ppb) (Table 6). Based on these two parameters, collected samples were plotted over a diagram created by Cowart and Osmond [43] to investigate possible applications of uranium isotopic analysis in groundwater samples in prospecting for various types of uranium ore bodies (Fig. 9).

All samples collected have low uranium content (< 1 ppb) which is indicative of reducing conditions or strata unusually low in uranium content [43]. If the pH and Eh data are plotted over a Pourbaix's Eh–pH diagram, then, it is possible to verify that the water samples are transitioning from slightly oxidizing tendencies typical of rain and surface water to mild and moderately reducing tendencies typical of groundwater, especially the ones collected at Caldas Novas city. Concerning to AR results, samples 20 and 26 have AR below 1, considered to be a low ratio and abnormal in groundwater because of the recoil effect. According to Cowart and Osmond [43], results like this can only be explained as a temporary (that is, on a 105 ka time scale) solution of absorbed uranium, i.e. the “remobilization of an accumulation”. Samples 1, 2, 3, 4, 8, 9, 11, 12, 17, 18, 19, 22, 24 and 25 have AR between 1 and 2, considered normal ratios and obtained by most researchers. Bonotto [20] states that the increase of ^{234}U in solution relates to the aquifer's degree of weathering since high values of AR are directly related to high rates of dissolution. Samples 5, 6, 10, 13, 14, 16 and 21 have AR above 2, which are high ratios. This is the result of the recoil process whereby the daughter ^{234}U atoms are injected into the solution independently of leaching effects.

Due to the low uranium content of these waters, only 5 samples with a concentration above 0.1 ppb are plotted in the graph, all of them from the dry season campaign. Sample 20 from the Hot Lagoon Park was classified as Reduced Groundwater ($U < 1$ ppb) with a Dispersing Accumulation ($AR < 1$), resulting in a “Mobile Accumulation Up-dip” situation, a category that rarely occurs according to Cowart and

Osmond [43]. Samples 18 and 22, also from the Hot Lagoon Park, are Reduced Groundwater ($U < 1$ ppb) with a Stable Accumulation ($1 < AR < 2$) resulting in a “Normal Down-dip Reduced Front”, as well as Sample 24 (Sulphur Spring). Sample 25, the single one from Rio Quente to plot on the diagram, was collected from the Esplanada Camping and is also a Reduced Groundwater ($U < 1$ ppb) with a Stable Accumulation ($1 < AR < 2$) resulting in a “Normal Down-dip from Reduced Front”. These results indicate that there are no potential uranium ore bodies currently forming by accumulation process from groundwater in the areas where samples were collected. Accumulations normally will exhibit high AR's near the ore body and surrounding regions, but this association is not necessarily congruent since high AR's are sometimes found in aquifers with no uranium accumulations as well [47].

Studies by Osmond et al. [48] have suggested the possibility of using AR and the inverse of uranium concentration ($1/U$) to determine the mixing volumes of different groundwater masses. The resulting pattern would be a linear variation in the case of 2 members, and a two-dimensional variation in the case of 3 or more members. Different patterns can be obtained as shown in Fig. 10 and possible interpretations are now pointed out.

Figure 10a shows a scatter plot with samples collected in the 2014 campaign, during the rainy season in the Caldas Novas Thermal Complex. In this scenario, the two-dimensional variation exhibits a four-sided polygon with samples 14, 16, 17 and 20 as vertices. Sample 14 was collected in the Pousada Costa Machado, a former lodging in south Caldas Novas. Samples 16 and 17 are both from the CTC Hotel in the central part of town and have the lowest uranium content and the highest temperature respectively. Sample 20 belongs to the Hot Lagoon Park, in the outskirts of town to the north-east, and has the highest uranium content among samples. All the other samples plotted inside the polygon, meaning their $1/U$ and AR values are resulting mixtures from springs at the vertices. Besides, samples inside the polygon are much closer to the Sample 20 vertex, indicating that this water is the dominant phase in the mixtures. This is probably due to lineaments of faults that control the drainage system underground and favors the occurrence of mixing processes towards NE where the Hot Lagoon Park is located.

Figure 10b shows a scatter plot with samples from the 2018 campaign during the dry season in the region, from which it was possible to tell apart two polygons. The first polygon is a vertically elongated triangle composed of samples 1–7 from the Hot Park in the Rio Quente Resorts. Samples 1–6 are hot springs while sample 7 is surface water that flows from the top of the Caldas Novas dome through the park. Vertices are composed of samples 1, 5 and 7 while samples 2, 3, 4 and 6 are plotted inside the triangle. Most samples plot closer to the Sample 1 vertex, indicating there

is a major influence from this spring on their composition. However, sample 6 shifted towards sample 7, which might indicate there has been a bigger influence of surface water in its composition.

The second polygon from Fig. 10b is a triangle composed of samples 10–13, all of them belonging to the Hot Lagoon Park in Caldas Novas city. This triangle is much wider horizontally, indicating that there is a greater variation in the uranium content of these samples. Sample 13 came from the Hot Lagoon, while samples 10 and 11 were collected from wells in the margins of the Pirapitinga River, represented by sample 12. The resulting water for Sample 11 was plotted halfway between springs 10 and 13, meaning that similar amounts of water contribute to the mixture. However, Sample 11 is much closer to the vertex of Sample 12, indicating significant proportions of fresh water are taking part in its mixture.

A linear variation was also observed for Fig. 10b in which Sample 8 plots over the pink dashed line that connects Samples 1 and 9. All samples were collected in Rio Quente city, Sample 1 being a hot spring from the Hot Park, Sample 8 collected from a channel that canalizes all waters from the park's domain, after appropriate treatment, for future disposal and Sample 9 collected from Camping Esplanada, a place that reuses the park's disposed water for recreational purposes. The proximity of Sample 8 to the vertex of Sample 1 shows that much of its composition relates to this hot spring, particularly in what concerns uranium content. The uranium content of Sample 9 is much diluted, being about 60 times smaller than Sample 1, which causes the resulting water to shift towards the left.

Figure 10c shows the variation observed for samples strictly from Rio Quente city. Samples 1–8 were collected directly from the Hot Park while samples 9, 25 and 26 were collected outside the park limits. The majority of samples exhibit a similar uranium concentration, apart from Sample 9, which shifted away to the right portion of the graph due to a much-diluted uranium content. Samples 5, 6 and 7 exhibited higher AR values and for that reason are plotted in the upper portion of the graph, which might indicate hot springs 5 and 6 are receiving some contribution of fresh water from river sample 7, or vice-versa. Samples 1–4 and 25 gathered closer to vertex 26, which seems to be a general tendency for those waters, all exhibiting similar uranium content and AR values greater than unit.

Figure 10d shows samples collected in Caldas Novas city, which were plotted inside a five-sided polygon and most of them exhibited relatively higher uranium content, reflected as a tendency to remain closer to the vertical axis. Additionally, samples 10, 11 and 12 from the Hot Lagoon Park were placed far off from the others, showing more diluted tendencies in what concerns the uranium content, despite being sampled during the dry season. Seasonality

shows that, in this scenario, samples collected from the very same springs over a four-year gap during different weather conditions exhibit contrasting behaviours. Only sample 13, collected from the Hot Lagoon in the dry season, exhibits similar behaviour to samples of the rainy season. A plausible hypothesis could be that sample 13 is placed further away from the Pirapitinga River (Sample 12) than samples 10 and 11, and receives little or no influence from fresh water.

Conclusions

Radon activity concentrations in the analyzed waters ranged from 0.365 to 60.779 Bq/L, and higher values are mostly associated with Caldas Novas city samples. The highest value almost reached the slightly radioactive class, according to the Brazilian Code of Mineral Waters. Anoxic and reducing environments directly influenced dissolved radon, especially in the presence of sodium. Uranium concentrations ranged from 0.001 to 0.308 $\mu\text{g/L}$, values far below from representing a health threat. Anoxic environments favored uranium concentrations, especially when pH ranged from neutral to slightly alkaline. An increase in electrical conductivity and calcium content were also linked to increasing uranium levels. Parameters influencing uranium are directly controlled by depth, indicating that higher U concentrations are coming from deep and confined aquifer regions with longer residence time, and revealing how the underground flow dynamics work in the area. Samples from Caldas Novas city with relatively higher uranium and radon content are circulating through deeper, reducing, alkaline environments, while Rio Quente samples with relatively lower uranium and radon content reflect a typical shallower, acidic water from oxidizing environments with short residence time. Dissolved uranium can exist predominantly in the form of uranyl carbonate complexes: UO_2CO_3 , $\text{UO}_2(\text{CO}_3)_2^{2-}$, $\text{UO}_2(\text{CO}_3)_3^{4-}$. The $^{234}\text{U}/^{238}\text{U}$ activity ratio in the waters ranged from 0.67 to 6.67 and was used as an indirect prospecting tool for uranium accumulations, but results indicate that there are no potential uranium ore bodies currently forming in the areas where samples were collected. Most of the water mixing processes occur due to fault systems in this intensely fractured terrain that control the underground flux and favor the occurrence of mixing processes. When analyzing samples from the perspective of different campaigns a noticeable contrast became evident. Seasonality showed that samples collected from the very same springs over a four-year gap during different weather conditions had contrasting behaviors, showing higher uranium content during the rainy season than in the dry season, when levels were paradoxically much diluted.

Acknowledgements The authors would like to thank the Coordination of Improvement of Higher Education Personnel (CAPES), Brazil, for the scholarship to ML and the Rio Quente Resorts Group, represented by Mrs Neide Tavares, for allowing the data acquisition in its domains. Two anonymous reviewers are greatly thanked for helpful comments that improved the readability of the manuscript.

Declarations

Conflict of interest The authors declare that they have no known competing financial interests or personal relationships that could have appeared to influence the work reported in this paper.

References

- Connecticut Department of Public Health (DPH) (2012) Radon in your water. Environmental Health Section. Radon Program. Fact Sheet February 2012 <https://sosradon.org/files/sosradon/resources/Connecticut%20Radon%20in%20Water.pdf> Accessed 08 Nov 2022
- World Health Organization (WHO) (2001) Depleted uranium: sources, exposure and health effects. Department of Protection of the Human Environment. Geneva April 2001 <https://www.who.int/publications/i/item/WHO-SDE-PHE-01.1> Accessed 08 Nov 2022
- Brazil (2011) Ministry of Health. Ordinance No. 2,914. Provides the procedures for controlling and monitoring the quality of water for human consumption and its potability standard. Brasília. Official Journal of the Union (DOU). 39–46. https://bvsmis.saude.gov.br/bvsmis/saudelegis/gm/2011/prt2914_12_12_2011.html Accessed 01 Sep 2022
- Brazil (1945) Code of Mineral Waters. Decree-Law No. 7.841 of August 8th 1945. https://www.camara.leg.br/proposicoesWeb/prop_mostrarintegra;jsessionid=C9B17DD08CE68890721582ECAFDBBDAD.proposicoesWebExterno2?codteor=439991&filename=LegislacaoCitada+-PL+282/2007 Accessed 14 Nov 2022
- USEPA (United States Environmental Protection Agency) (2022) National Primary Drinking Water Regulations (NPDWR) https://www.epa.gov/sites/default/files/2016-06/documents/npdr_complete_table.pdf Accessed 18 Jul 2022
- USGS (United States Geological Survey) (1962) Data on uranium and radium in ground water in the United States, 1954 to 1957. Washington, U.S. Govt Print Off <https://pubs.usgs.gov/pp/0426/report.pdf> Accessed 18 Jul 2022
- WHO (World Health Organization) (2017) Guidelines for drinking-water quality: 4th Edition incorporating the 1st addendum. <https://www.who.int/publications/i/item/9789241549950> Accessed 18 Jul 2022
- Catão RLCMR, Feitosa PHC, Rodrigues ACL, Barbosa DL, Guedes MTJC (2022) Maximum recommended and allowable radon-222 limits in water and air: systematic review. <https://doi.org/10.21203/rs.3.rs-1280942/v1>
- USEPA (United States Environmental Protection Agency) (2014) Basic information about radon in drinking water. <https://archive.epa.gov/water/archive/web/html/basicinformation-2.html> Accessed 10 Nov 2022
- Swistock B (2022) Reducing radon in drinking water. College of Agricultural Sciences. Pennsylvania State University <https://extension.psu.edu/reducing-radon-in-drinkingwater#:~:text=Based%20on%20the%20potential%20for,but%20no%20standard%20currently%20exists.> Accessed 10 Nov 2022
- EU Commission Recommendation (2001), (2001/928/Euratom), Commission Recommendation of 20 December 2001 on the protection of the public against exposure to radon in drinking water supplies (notified under document number C(2001) 4580) OJ L 344, 28.12.2001, p. 85–88 <https://eur-lex.europa.eu/eli/reco/2001/928/oj> Accessed 08 Nov 2022
- Gruber V, Ringer W (2017) Radon exposure at specific workplaces in Austria—experiences and future challenges. *Radiat Prot Dosim* 177:7–11
- Godoy JM, Godoy ML (2006) Natural radioactivity in Brazilian groundwater. *J Environ Radioact*. <https://doi.org/10.1016/j.jenvrad.2005.05.009>
- Campos EC, Costa JFG, Marques JDM (1980) Hydrogeological Study Project of the Caldas Nova Region, Goiás. <https://rigeo.cprm.gov.br/xmlui/handle/doc/9259> Accessed 01 Sep 2022
- Cook PG, Favreau G, Dighton JC, Tickell C (2003) Determining natural groundwater influx to a tropical river using radon, chloro-fluorocarbons and ionic environmental tracers. *J Hydrol*. [https://doi.org/10.1016/S0022-1694\(03\)00087-8](https://doi.org/10.1016/S0022-1694(03)00087-8)
- Fianco ACB (2011) Radon concentrations in groundwater, rocks and soils in Porto Alegre (RS). Master's thesis. <https://www.lume.ufrgs.br/bitstream/handle/10183/32667/000786610.pdf?sequence=1> Accessed 01 Sep 2022
- Fleischer RL (1980) Isotopic disequilibrium of uranium: Alpha-recoil damage and preferential solution effects. *Science* 207(4434):979–981. <https://doi.org/10.1126/science.207.4434.979>
- Skeppström K, Olofsson B (2007) Uranium and radon in groundwater: an overview of the problem. *Eur Water* 17(18):51–62
- Tanner AB (1980) Radon migration in the ground: a supplementary review. Natural Radiation Environment III, Symp. Proc., US DOE, NTIS Report CONF-780422 1 5–56 https://inis.iaea.org/search/search.aspx?orig_q=RN:12618303 Accessed 17 Nov 2022
- Bonotto DM (2004) Radioactivity in waters: from England to Guarani. UNESP, São Paulo, São Paulo.
- Silveira EG, Bonotto DM (1995) Hydrogeochemical behavior of uranium isotopes in Águas de Lindóia (SP), Brazil. *Braz J Geol* 25(3):165–172
- Ivanovich M, Harmon RS (1992) Uranium-series disequilibrium. Clarendon Press, Oxford
- Bonotto DM (1993) Enhancement of uranium 234 in springwaters of Águas da Prata, São Paulo, Brazil. *Water Resour Res*. <https://doi.org/10.1029/93WR00607>
- INB (Nuclear Industries of Brazil) (2022) Resources <http://www.inb.gov.br/en-us/Our-Activities/Uranium/Resources> Accessed 18 Jul 2022
- World Nuclear Association (2022) Nuclear Power in Brazil <https://world-nuclear.org/information-library/country-profiles/countries-a-f/brazil.aspx> Accessed 18 Jul 2022
- IAEA (International Atomic Energy Agency) (2009) World Distribution of Uranium Deposits (UDEPO) with Uranium Deposit Classification https://www-pub.iaea.org/MTCD/publications/PDF/TE_1629_web.pdf Accessed 18 Jul 2022
- World Nuclear Association (2020) Geology of Uranium Deposits <https://world-nuclear.org/information-library/nuclear-fuel-cycle/uranium-resources/geology-of-uranium-deposits.aspx> Accessed 18 Jul 2022
- Lunardi M, Bonotto DM (2018) Hydrochemical study of the Caldas Novas Thermal Complex (GO), Brazil. *Environ Earth Sci*. <https://doi.org/10.1007/s12665-018-7240-x>
- Campos JEG, Tröger U, Haesbaert FF (2005) Caldas Novas hot spring, State of Goiás: remarkable occurrence of thermal water not related to magmatism. <https://sigep.eco.br/sitio113/sitio113english.pdf> Accessed 18 Jul 2022
- Carlos PMS (2017) Radioactivity in waters intended for human consumption. Master's Thesis. Coimbra Polytechnic Institute.

- https://comum.rcaap.pt/bitstream/10400.26/20896/1/Radioatividade%20nas%20C3%A1guas%20destinadas%20a%20consumo%20humano_Pedro%20Carlos_%20MGA_2017.pdf Accessed 01 Sep 2022
31. Durrige Radon Instrumentation (2017) RAD7 Radon Detector User Manual. (Durrige Company Inc. USA) www.durrige.com/documentation/RAD7%20Manual.pdf Accessed 28 Jul 2022
 32. Lunardi M (2016) Hydrochemical study of the Caldas Novas Thermal Complex (GO), Brazil. Master's thesis. São Paulo State University. Rio Claro <https://repositorio.unesp.br/handle/11449/144662> Accessed 01 Sep 2022
 33. Campbell Scientific Inc (2009) Interfacing the AlphaGUARD Radon Monitor with Campbell Scientific's CR1000 Datalogger <https://s.campbellsci.com/documents/us/technical-papers/alpha-guard.pdf> Accessed 28 Jul 2022
 34. WHO (World Health Organization) (2017) Guidelines for drinking-water quality: 4th Edition incorporating the 1st addendum. <https://www.who.int/publications/i/item/9789241549950> Accessed 18 Jul 2022
 35. Salim LA (2013) Use of RAD7 for characterizing thoron in spa waters. Master's thesis. São Paulo State University. Rio Claro <https://repositorio.unesp.br/handle/11449/92726> Accessed 01 Sep 2022
 36. Barbosa EQ (2013) Radon as an indicator of soil contamination by hydrocarbons. Monography. São Paulo State University. Rio Claro <https://repositorio.unesp.br/handle/11449/118200> Accessed 01 Sep 2022
 37. Thomazini FO, Cigagna C, Bonotto DM (2015) A comparative method for evaluating the natural uranium isotopes ^{238}U and ^{234}U in waters <https://repositorio.unesp.br/handle/11449/172561> Accessed 04 Aug 2022
 38. Laerd Statistics (2020) Pearson's product moment correlation. Statistical tutorials and software guides. <https://statistics.laerd.com/statistical-guides/pearson-correlation-coefficient-statistical-guide.php> Accessed 16 Nov 2022
 39. Laerd Statistics (2020) Hypothesis testing. Statistical tutorials and software guides. <https://statistics.laerd.com/statistical-guides/hypothesis-testing-3.php> Accessed 16 Nov 2022
 40. McLeod SA (2019) What a p-value tells you about statistical significance. Simply Psychology www.simplypsychology.org/p-value.html Accessed 16 Nov 2022
 41. Bonotto DM, Bueno TO (2008) The natural radioactivity in Guarani aquifer groundwater, Brazil. *Appl Radiat Isot.* <https://doi.org/10.1016/j.apradiso.2008.03.008>
 42. Langmuir D (1978) Uranium solution-mineral equilibria at low temperatures with applications to sedimentary ore deposits. *Geochim Cosmochim Acta.* [https://doi.org/10.1016/0016-7037\(78\)90001-7](https://doi.org/10.1016/0016-7037(78)90001-7)
 43. Cowart JB, Osmond JK (1980) Uranium isotopes in ground water as a prospecting technique. Florida State Univ., Tallahassee (USA). <https://doi.org/10.2172/5418440>
 44. Cumberland SA, Douglas G, Grice K, Moreau JW (2016) Uranium mobility in organic matter-rich sediments: a review of geological and geochemical processes. *Earth-Sci Rev* 159(2016):160–185. <https://doi.org/10.1016/j.earscirev.2016.05.010>
 45. Baik MH, Jung EC, Jeong J (2015) Determination of uranium concentration and speciation in natural granitic groundwater using TRIFS. *J Radioanal Nucl Chem* 305(2):589–598. <https://doi.org/10.1007/s10967-015-3971-2>
 46. Zhou P, Gu BH (2005) Extraction of oxidized and reduced forms of uranium from contaminated soils: effects of carbonate concentration and pH. *Environ Sci Technol* 39(12):4435–4440. <https://doi.org/10.1021/es0483443>
 47. Osmond JK, Cowart JB (1976) The theory and uses of natural uranium isotopic variations in hydrology. *At Energy Rev* 14(4):621–679
 48. Osmond JK, Kaufman MI, Cowart JB (1974) Mixing volume calculations, sources and aging trends of Floridan aquifer water by uranium isotopic methods. *Geochim Cosmochim Acta.* [https://doi.org/10.1016/0016-7037\(74\)90006-4](https://doi.org/10.1016/0016-7037(74)90006-4)

Publisher's Note Springer Nature remains neutral with regard to jurisdictional claims in published maps and institutional affiliations.

Springer Nature or its licensor (e.g. a society or other partner) holds exclusive rights to this article under a publishing agreement with the author(s) or other rightsholder(s); author self-archiving of the accepted manuscript version of this article is solely governed by the terms of such publishing agreement and applicable law.